Available online at www.sciencedirect.com

ScienceDirect

IFAC Papers Online CONFERENCE PAPER ARCHIVE

IFAC PapersOnLine 54-16 (2021) 132–138

Deep Integration of INS and DP: from Theory to Experiments

Elena Ambrosovskaya [*,**] **Dmitry Romaev** [*]
Anton Proskurnikov [***] **Andrey Loginov** [*]
Alexander Mordvintsev [*] **Alexander Miroshnikov** [*,**]
Igor Fedorov [****]

[*] *Navis Engineering OY, St. Petersburg R&D Center, Russia*
[**] *St. Petersburg Electrotechnical University "LETI", Russia*
[***] *Politecnico di Torino, Italy*
[****] *SIA Fiber Optical Solution, Latvia*

Abstract: The recent progress of measurement devices and algorithms of inertial navigation opens up the perspective of deep integration between inertial navigation systems (INS) and dynamic positioning (DP) systems. In the literature, novel mathematical algorithms for INS-guided sensor fusion and sensor fault isolation have recently been proposed, aimed primarily at robust and resilient observation of the vessel's attitude and position. Much less has been done for experimental testing of INS-guided DP systems in real environmental conditions. In this paper, we report experimental results (from bench tests to real sea trials), demonstrating the efficacy of a fiber-optic inertial measurement sensor in a real DP system. Besides this, we discuss some new applications of INS systems in DP operations and relevant mathematical algorithms.

Keywords: Dynamic positioning, inertial navigation, ship motion control, sensor fusion

1. INTRODUCTION

The standard set of sensors for dynamic positioning (DP) includes position references, gyrocompasses, wind sensors and motion reference units (ABS, 2013). In parallel with DP, the technologies of inertial navigation systems (INS) was developing (King, 1998; Titterton and Weston, 2004). The progress in electronics and fiber optics has yielded precise, reliable and relatively cheap inertial measurement units (IMU). This enables to implement long-standing plans of using INS into DP operations as an additional sensor (Vickery, 1999; Stephens et al., 2008; Carter, 2011). Mathematical results, reported in systems and control literature, suggest that the additional inertial sensor allows to increase the precision of the vessel's attitude and position estimates (Hua, 2010; Grip et al., 2015; Bryne et al., 2018), increasing the sensors' redundancy Bryne et al. (2017), enabling fault isolation (Rogne et al., 2014) and operations in the position "dead reckoning" mode (Rogne et al., 2016). However, the experimental results showing that existing INS are instrumental in DP operations are quite limited and mainly concerned with development of new sensors, integrating INS and position references (Paturel, 2014; Russell, 2012; Rinnan et al., 2012).

The R&D center of Navis Engineering OY company works on deep integration of an INS into **Navis NavDP 4000** DP control system [2]. As an inertial measurement unit (IMU), we use a precise fiber-optic device IFOS-500 manufactured by Fiber Optical Solution. [3] IFOS-500 provides RS-422 interface and is connected to the control computer through the interface box (Fig. 1) collecting sensors' data.

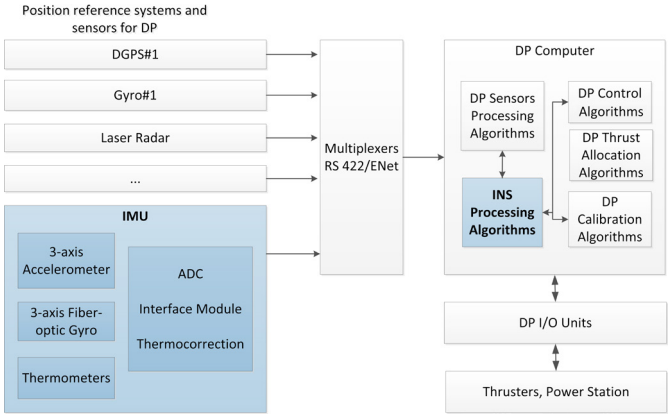

Fig. 1. Integration of the INS and the DP control system

Potential applications of the INS in DP operations, along with the aforementioned vessel's state vector estimation, fault isolation and operations in dead reckoning modes, include estimation of the external forces and online tuning of the vessel's mathematical models. In this paper, we report our progress in these problems and the results of experiments (including seatrials on a real vessel).

[1] Email: {e.ambrosovskaya,d.romaev,a.loginov,a.mordvintsev,-a.miroshnikov}@navisincontrol.com, anton.p.1982@ieee.org, iv_fedorov@optolink.ru

[2] https://navisincontrol.com/upload/iblock/c67/New-DP-broshure_2.pdf

[3] http://opticalsolution.lv/products/inertial-measurement-units/

10.1016/j.ifacol.2021.10.084

2. VESSEL MOTION ESTIMATION

The reference frames (Fig. 2) associated with a ship are (Titterton and Weston, 2004, Section 3.3):

- The *inertial* frame**[i]** has its origin at the centre of the Earth and axes which are non-rotating with respect to the fixed stars;
- The frame **[e]** has its origin at the centre of the Earth and axes which are fixed with respect to the Earth;
- The North-East-Down, or navigation frame **[n]** has its origin at the location of the navigation system, point P, and axes aligned with the directions of north, east and the local vertical (down);
- The forward-starboard-down, or body frame **[b]** is an orthogonal axis set which is aligned with the roll, pitch and yaw axes of the vessel in which the navigation system is installed.

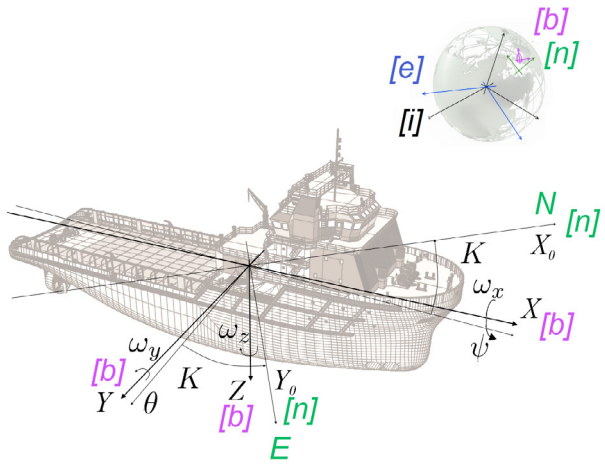

Fig. 2. Coordinate systems associated to the vessel.

Henceforth, we use **bold** font for rotation matrices, 3-dimensional physical vectors (velocity, acceleration, angular velocity) and their coordinate representations. Scalars and coordinate vectors that do not correspond to any physical vector are denoted by normal font.

The coordinates of an arbitrary physical vector (velocity, acceleration etc.) $\mathbf{z}$ in the frame [f] (where $f = i, e, n, b$) are henceforth denoted by $\mathbf{z}^f := [z_x^f, z_y^f, z_z^f]^\top$. We use $\boldsymbol{\omega}_{gh}$ to denote the angular velocity of rotation of frame [h] with respect to frame [g]; it is well known that $\boldsymbol{\omega}_{fh} = \boldsymbol{\omega}_{fg} + \boldsymbol{\omega}_{gh}$. The symbol $\mathbf{R}_h^g$ stands for the rotation matrix transforming frame [g] into frame [h]. It is well known that

$$\mathbf{z}^g = \mathbf{R}_h^g z^h, \quad \mathbf{R}_h^g = (\mathbf{R}_g^h)^\top = (\mathbf{R}_g^h)^{-1}$$

for any vector $\mathbf{z}$ and pair of frames [g],[h].

Given a coordinate vector $x \in \mathbb{R}^3$, we use $[x\times]$ to denote the skew-symmetric matrix of cross product associated with it: $x \times y = [x\times]y$ whenever $y \in \mathbb{R}^3$. For an arbitrary frame [f] and two physical vectors $\mathbf{z}, \mathbf{w}$ we have

$$(\mathbf{z} \times \mathbf{w})^f = [\mathbf{z}^f\times]\mathbf{w}^f = -[\mathbf{w}^f\times]\mathbf{z}^f.$$

It can be shown that if $\mathbf{R}$ is a rotation 3×3 matrix, then

$$\mathbf{R}[x\times]y = [\mathbf{R}x\times]\mathbf{R}y \Longleftrightarrow [x\times] = \mathbf{R}^\top[\mathbf{R}x\times]\mathbf{R}\,\forall x, y \in \mathbb{R}^3.$$

Replacing here $\mathbf{R}$ by $\mathbf{R}^\top$, the latter equality shapes into

$$[x\times]\mathbf{R} = \mathbf{R}[\mathbf{R}^\top x\times]. \tag{1}$$

The following relation between the rotation matrices and angular velocities is also well known

$$\dot{\mathbf{R}}_g^f = [\boldsymbol{\omega}_{fg}^f\times]\mathbf{R}_g^f = \mathbf{R}_g^f[\boldsymbol{\omega}_{fg}^g\times]. \tag{2}$$

2.1 The IMU measurements and data processing

Characteristics of the IMU are summarized in Appendix A. The structural diagram of data processing system is shown in Fig. 3.

The inertial sensor measures the absolute acceleration (with respect to the inertial frame) created by all non-gravitational forces $\mathbf{a} - \mathbf{g}$ and the absolute (inertial) angular velocity of the frame [b]. Coordinates of both physical vectors are written the frame [b]. Taking into account the *measurement noises* ξ_a, ξ_ω, the two coordinate vectors received from the sensor are

$$a_{imu}(t) = \mathbf{a}^b(t) - \mathbf{g}^b(t) + \xi_a(t) \in \mathbb{R}^3,$$
$$\omega_{imu}(t) = \boldsymbol{\omega}_{ib}^b(t) + \xi_\omega(t) \in \mathbb{R}^3.$$

The noises can be decomposed into slowly changing *bias* components $a_0(t), \omega_0(t)$ (that are considered as almost constant and depend on the temperature and internal sensor's parameters) and a small high-frequency noise. The corrected measurements used to estimate the vessel's velocity and position are therefore

$$\bar{a}(t) = a_{imu}(t) - a_0(t) \approx \mathbf{a}^b(t) - \mathbf{g}^b(t) \tag{3}$$
$$\bar{\omega}(t) = \omega_{imu}(t) - \omega_0(t) \approx \boldsymbol{\omega}_{ib}^b(t), \tag{4}$$

where $\approx$ means "equals modulo small high-frequency noises (that can be rejected by low-pass filtering)".

The equations of motion to be integrated involve the following variables (we work in the navigational frame [n], where the relations between the position, ground velocity and the Earth angular velocities are simpler):

- the rotation matrix $\mathbf{R}_b^n$;
- the vector of *ground* vessel's velocity written in the frame [n] $\mathbf{v}_e^n = (v_N, v_E, v_D)^\top$;
- the coordinate vector of the vessel's position $\rho = (\varphi, \lambda, h)^T$, where φ is the latitude, λ is the longitude and h is the height [4];
- the vector of gravity acceleration $\mathbf{g}^n = (0, 0, g_s)^\top$ at the vessel's position;
- the angular velocities $\boldsymbol{\omega}_{ie}^n$ (rotation of the Earth) and $\boldsymbol{\omega}_{en}$; obviously, $\boldsymbol{\omega}_{in} = \boldsymbol{\omega}_{ie} + \boldsymbol{\omega}_{en}$.

The equation for the rotation matrix (Poisson equation) is as follows

$$\begin{aligned}\dot{\mathbf{R}}_b^n \overset{(2)}{=} \mathbf{R}_b^n[\boldsymbol{\omega}_{nb}^b\times] = \mathbf{R}_b^n[\boldsymbol{\omega}_{ib}^b\times] - \mathbf{R}_b^n[\boldsymbol{\omega}_{in}^b\times] \overset{(1),(2)}{=} \\ = \mathbf{R}_b^n[\boldsymbol{\omega}_{ib}^b\times] - [\boldsymbol{\omega}_{in}^n\times]\mathbf{R}_b^n \overset{(4)}{=} \\ = \mathbf{R}_b^n[(\omega_{imu}(t) - \omega_0(t))\times] - [(\boldsymbol{\omega}_{ie}^n + \boldsymbol{\omega}_{en}^n)\times]\mathbf{R}_b^n.\end{aligned} \tag{5}$$

The vector of the vessel's ground speed evolves as follows (Titterton and Weston, 2004, Eq. 3.22)

$$\begin{aligned}\dot{\mathbf{v}}_e^n = \mathbf{R}_b^n(\mathbf{a}^b - \mathbf{g}^b) - (2\boldsymbol{\omega}_{ie}^n + \boldsymbol{\omega}_{en}^n) \times \mathbf{v}_e^n + \mathbf{g}^n = \\ = \mathbf{R}_b^n(a_{imu}(t) - a_0(t)) - (2\boldsymbol{\omega}_{ie}^n + \boldsymbol{\omega}_{en}^n) \times \mathbf{v}_e^n + \mathbf{g}^n.\end{aligned} \tag{6}$$

The vessel's position in the geographic coordinates evolves as (Titterton and Weston, 2004, Section 3.7)

$$\dot{\rho}(t) = \left[\frac{v_N}{M_\oplus(\varphi)}, \frac{v_E}{N_\oplus(\varphi)\cos\varphi}, v_D\right]^T, \tag{7}$$

[4] Note: ρ is not a geometric vector, but just a triple of numbers.

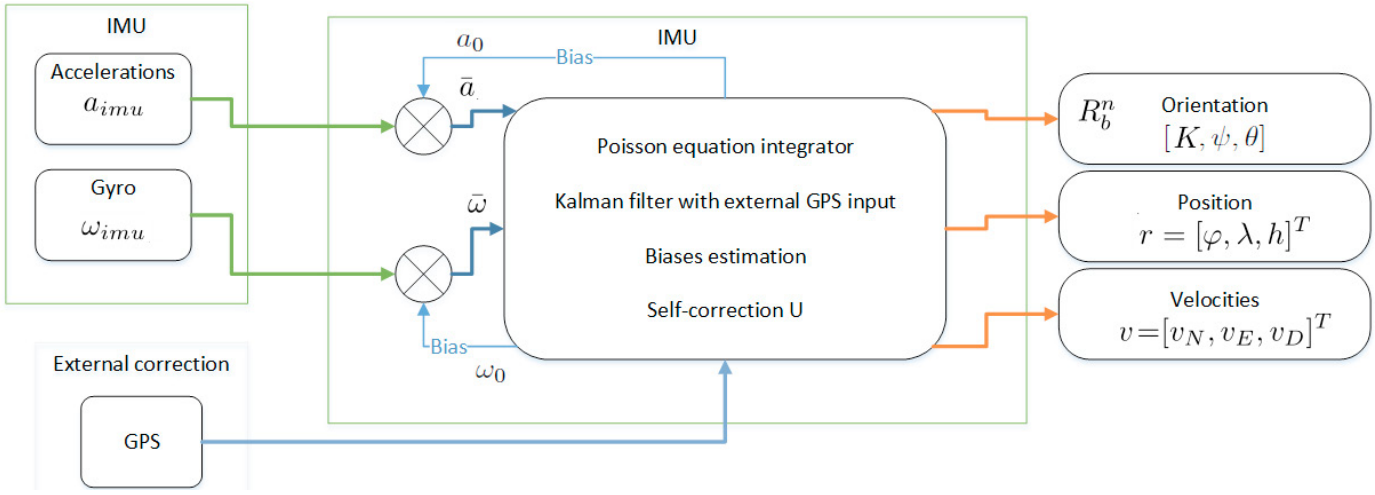

Fig. 3. INS data processing: a structural scheme.

where $M_\oplus(\varphi)$ is the meridian Earth radius and $N_\oplus(\varphi)$ is the transverse radius of curvature. Recall that the biases ω_0, a_0 are supposed to be slowly changing, so

$$\dot{\omega}_0 = \dot{a}_0 = 0. \tag{8}$$

To close the system of equations, one needs the representation of two angular velocities in the frame [n], which is found as follows (Titterton and Weston, 2004, Section 3.7)

$$\boldsymbol{\omega}_{ie}^n = \Omega \begin{pmatrix} \cos\varphi \\ 0 \\ -\sin\varphi \end{pmatrix}, \quad \boldsymbol{\omega}_{en}^n = \begin{pmatrix} v_E/N_\oplus(\varphi) \\ -v_N/M_\oplus(\varphi) \\ -v_E \tan\varphi/N_\oplus(\varphi) \end{pmatrix}, \tag{9}$$

where $\Omega = |\boldsymbol{\omega}_{ie}|$ is the Earth's absolute rotation rate (with respect to the polar axis).

2.2 Integration of the equations: two-stage estimation procedure

The direct integration of Eqs. (5)-(9) is impossible for two reasons: first, we do not know the exact initial position and heading of the vessel, second, the sensor's biases are unknown. The standard approach to solution estimation is to use an *observer* whose structure is borrowed from (Matveev and Raspopov, 2009). The observer's equation involve *estimates* of the variables $\mathbf{R}_b^n(t), \mathbf{v}_e^n(t), \rho(t), \omega_0(t), a_0(t)$ (we denote them, respectively, by $\tilde{\mathbf{R}}(t), \tilde{v}(t), \tilde{\rho}(t), \tilde{\omega}_0(t), \tilde{a}_0(t)$) and the vector of correction terms $U = (u_\beta, u_v, u_\rho, u_{\omega_0}, u_{a_0})^\top$. The elements of the velocity and position estimates are denoted as

$$\tilde{v} = (\tilde{v}_N, \tilde{v}_E, \tilde{v}_D), \quad \tilde{\rho} = (\tilde{\varphi}, \tilde{\lambda}, \tilde{h}).$$

The dynamics of the estimates are as follows

$$\begin{aligned}
\dot{\tilde{\mathbf{R}}} &= \tilde{\mathbf{R}}[(\omega_{imu} - \tilde{\omega}_0)\times] - [(\tilde{\omega}_{ie}^n + \tilde{\omega}_{en}^n + u_\beta)\times]\tilde{R} \\
\dot{\tilde{v}} &= \tilde{\mathbf{R}}(a_{imu} - \tilde{a}_0) - (2\tilde{\omega}_{ie}^n + \tilde{\omega}_{en}^n) \times \tilde{v} + \mathbf{g}^n + u_v, \\
\dot{\tilde{\rho}} &= \left[\frac{\tilde{v}_N}{M_\oplus(\tilde{\varphi})}, \frac{\tilde{v}_E}{N_\oplus(\tilde{\varphi})\cos\tilde{\varphi}}, \tilde{v}_D\right]^T + u_\rho, \\
\dot{\tilde{\omega}}_0 &= u_{\omega_0}, \quad \dot{\tilde{a}}_0 = u_{a_0},
\end{aligned}$$

Notice that $\mathbf{g}^n$ and the measurements a_{imu}, ω_{imu} are known and $\tilde{\omega}_{ie}^n, \tilde{\omega}_{en}^n$ are found by substituting $\tilde{\varphi}$ into (9). It can also be shown that $\tilde{\mathbf{R}}$ is a rotation matrix provided that the initial condition $\tilde{\mathbf{R}}(0)$ is a rotation matrix.

2.3 Reference-aided data processing: estimation errors

The dynamics of observation errors can be represented as a set of differential equations

$$\frac{d}{dt}\begin{pmatrix} \beta \\ \Delta v \\ \Delta\rho \\ \Delta\omega_0 \\ \Delta a_0 \end{pmatrix} = \begin{pmatrix} -[\tilde{\omega}_{in}^n\times] & S_\omega^v & S_\omega^r & -\tilde{\mathbf{R}} & 0 \\ [(\tilde{\mathbf{R}}a_{imu})\times] & S_v^v & S_v^r & 0 & \tilde{R} \\ 0 & S_r^v & S_r^r & 0 & 0 \\ 0 & 0 & 0 & 0 & 0 \\ 0 & 0 & 0 & 0 & 0 \end{pmatrix} \begin{pmatrix} \beta \\ \Delta v \\ \Delta\rho \\ \Delta\omega_0 \\ \Delta a_0 \end{pmatrix} + \begin{pmatrix} u_\beta + S_\omega^u u_\rho \\ u_v + \tilde{v} \times (S_\omega^u u_\rho) \\ u_\rho \\ u_{\omega_0} \\ u_{a_0} \end{pmatrix}.$$

Here S_ω^v, S_ω^r, S_ω^u, S_v^v, S_v^r, S_r^v, S_r^r are matrix coefficients (that can be found explicitly), $\Delta v = \tilde{v} - \mathbf{v}_e^n$, $\Delta\rho = \tilde{\rho} - \rho$, $\Delta\omega_0 = \tilde{\omega}_0 - \omega_0$, $\Delta a_0 = \tilde{a}_0 - a_0$ and vector β is defined as

$$[\beta\times] = \tilde{\mathbf{R}}(\mathbf{R}_b^n)^\top - I,$$

which is considered as a discrepancy between the observed and actual rotation matrices (I is the 3×3 identity matrix).

If the vector of discrepancies $\Delta x = [\beta, \Delta v, \Delta\rho, \Delta\omega_0, \Delta a_0]^\top$ was measured, the correcting terms U could be found as a simple "PI controller"

$$u_\beta = -k_\beta\beta, \quad u_\rho = -k_\rho\Delta\rho, \tag{10}$$

$$u_{\omega_0} = -k_{\omega 0}\Delta\omega_0, \quad u_{a_0} = -k_{a0}\Delta a_0, \tag{11}$$

$$u_v = -k_v\Delta v - k_{v,i}\int \Delta v. \tag{12}$$

However, the whole discrepancy vector (equivalently of course cannot be measured). In the normal situation (GPS data are available), we can measure the vector of position ρ (which allows to find $\Delta\rho$) and/or the ground velocity (course and speed over ground) $\mathbf{v}_e^n$ (allowing to find Δv). The remaining components are recovered by using the extended Kalman filter (EKF) of order 15. In the absence of GPS measurements, manual input of the vessel's position is possible (as used, for instance, in the testbench experiment described below). In the case of dead reckoning, the sensor is updated by zero velocity.

2.4 Experiments on a testbed and a real vessel.

Since it is difficult to compare fast-oscillating signals, sophisticated maneuvers are needed to compare measurements of different pitch/roll sensors. During these maneuvers, accelerations in x-,y- and yaw directions are given.

Picth/roll estimation results. For experiments, we use a platform equipped with sensors and computer (Fig. 4). This platform can be considered as a pendulum of 2.3m length (natural period is about 3 sec). During the experiments, the INS filter is "zero-aided", that is, it receives the constant latitude and longitude of the testbench location (oscillations of the platform are ignored).

In Fig. 5, the results of pitch and roll estimation during the aforementioned testbench are shown. We compare Navis INS (3) with two different MRU sensors (1 and 2). The accuracies of the pitch and roll estimates are within 0.1°.

Fig. 4. Pitch/roll estimation testbench

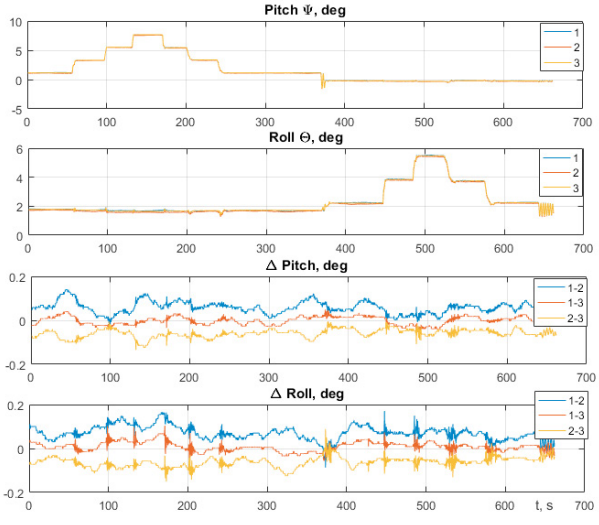

Fig. 5. Pitch/roll estimation (steps), testbench

Heading estimation results. In Fig. 6, we compare the estimated vessel's heading with gyrocompasses. The measurements have been collected during the seatrials of an icebreaking vessel (Appendix B). Starting vessel at almost zero speed and constant heading, the heading estimate is ready in about 5-15 minutes and has approximately same quality as navigation gyrocompasses.

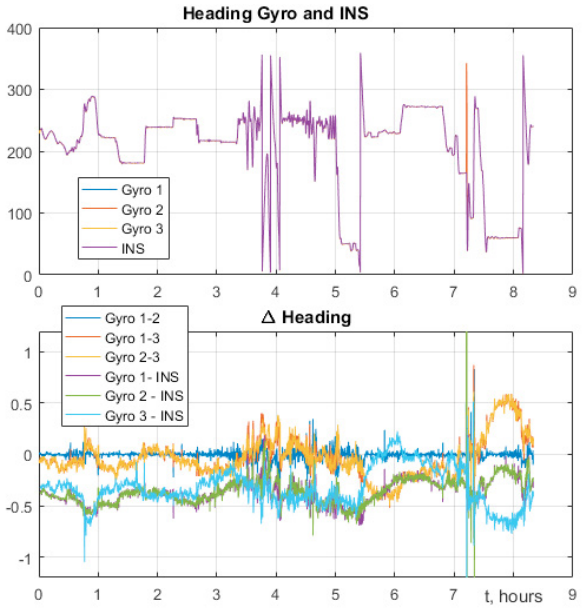

Fig. 6. Heading estimation and errors, sea trials

3. FORCES AND MOMENTS ESTIMATION

During DP control system calibration or verification (annual trials), one of the problems is to calibrate the forces and moments of the vessel's actuators using special maneuvers (Ambrosovsky and Ambrosovskaya, 2005). In the simplest situation (fixed-pitch propeller or tunnel thruster), such a calibration requires to tune a single *correction coefficient* for the thruster, that is, the ratio between the actual and the nominal forces. Calibration of CPP propellers, rotational thrusters and rudders is more delicate, because the correction coefficient, in general, depends on the propeller's pitch and/or the thrust direction.

Traditionally, offline frequency-domain procedures are used to estimate accelerations. Usage of direct acceleration measurements, provided by INS, can simplify this process and, furthermore, provide an online calibration tool for DP operators. Impulsive external forces can also be estimated.

3.1 The estimator of forces and yaw moment

The forces estimator (Fig. 7) includes:

(1) Nonlinear filter provides median filtering of raw acceleration measurements a_x, a_y (sampled at 600Hz) with subsequent and moving averaging. Fig. 8 shows the result of online X-acceleration filtering.
(2) Nonlinear differentiating filter to estimate the yaw acceleration $\dot{\omega}_z$.
(3) Actual forces are determined by the mass, added masses and accelerations $F_{x\ sum} = (m + m_{11})a_x$, $F_{y\ sum} = (m + m_{22})a_y$, $M_{z\ sum} = (J_z + m_{66})\omega_z$.
(4) Estimator of "nominal" forces (based on actuator commands and feedbacks); these nominal forces can be compared with estimated *actual forces* F_{sum} to compute correction coefficients.

(5) Estimator of external forces and their corresponding arms, which can be found from the relation

$$F_{sum} = F_{thr} + F_{hydro} + F_{aero} + F_{external}$$

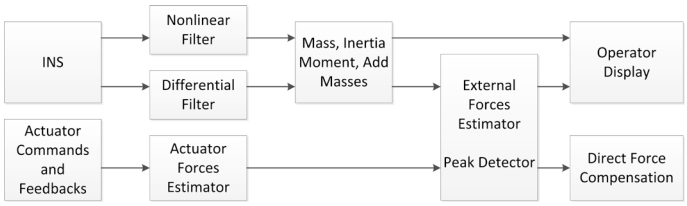

Fig. 7. Forces estimation scheme

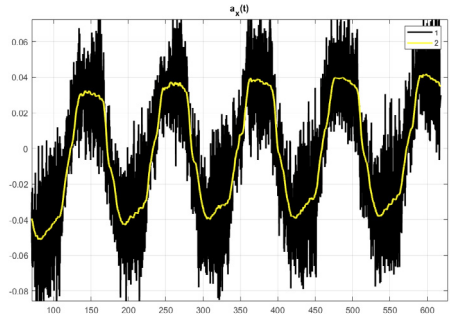

Fig. 8. Filtered acceleration

3.2 Experiments

Fig. 9 demonstrates the results of online X-force estimation (INS, command force and feedback force estimations) during the longitudinal calibration maneuver. Fig. 10 shows the result of online yaw moment estimation (INS, command force and feedback force estimations) during the rotation calibration maneuver. All data are obtained during seatrials of an icebreaking vessel (whose particulars are summarized in Section B). Comparing the nominal (bollard pull) forces estimated from the thrusters' feedbacks and the actual forces given by INS, the correction coefficient for each thruster can be obtained.

Fig. 11 demonstrates windows of **Navis NavDP 4000** control system, displaying the estimated generalized forces and the vessel's position on a map during test maneuvers.

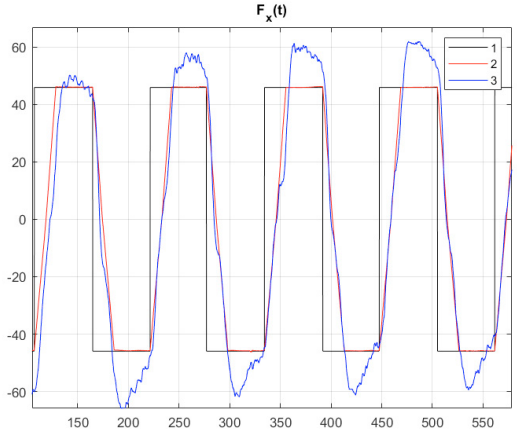

Fig. 9. X-Forces: commanded (1), feedback (2), estimate from INS (3)

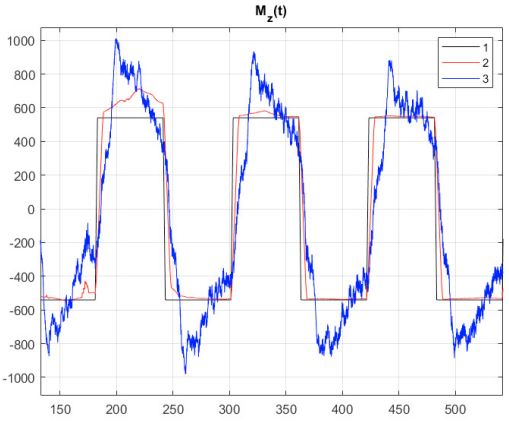

Fig. 10. Yaw Moments: commanded (1), feedback (2), estimate from INS (3)

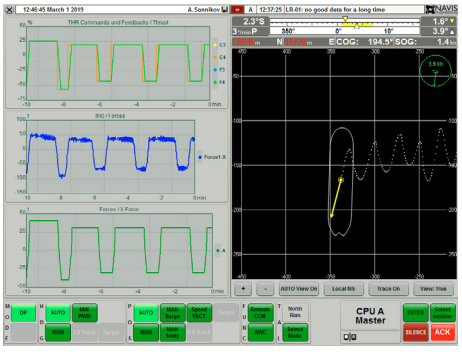

Fig. 11. **Navis NavDP 4000** windows: thrusters commands and forces, the vessel's trace.

To investigate possibility of estimation and compensation of single ice floes impact on vessel hull (open ice conditions) a joint study with Aker Arctic was conducted. Aker Arctic facilities for study includes Ice Towing Tank (Fig. 12) and a scaled model of an icebreaker with extended telemetry system for local hull positioning. For the experiments, this model was additionally equipped with the IMU sensor and the interface with Navis NavDP 4000 system. External forces can be applied manually at different points of the vessel (Fig. 13) to simulate ice impact.

Fig. 12. Towing tank tests with Aker Arctic (Polaris icebreaker model), January 2019

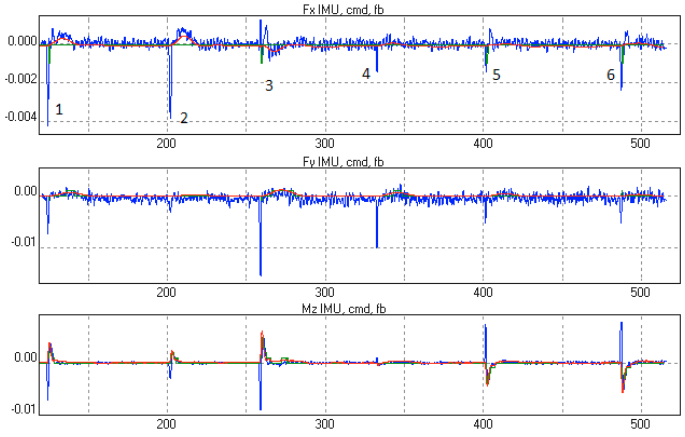

Fig. 13. External Force action

Assuming a simple model of impact process, the point of impact can be found by finding a minimum of the least-square "error"

$$[l_x, l_y] = argmin\{\sum\big[l_x F_y(t) - l_y F_x(t) - M_z(t)\big]^2\}$$

over all possible points (l_x, l_y) on the vessel's waterline.

Our experiments have shown that in reality a simpler least-square problem gives a good approximation of the x-arm

$$[l_x] = argmin\{\sum\big[l_x F_y(t) - M_z\big]^2\}.$$

The above formulation provides estimation of the impact point location on the waterline. It was found that this simplified approach provides a more robust estimation of external impact point and direction in real time. For the experiment in Fig. 13 the following data were estimated:

Experiment	Starting Time, s	Direction estimate, °	x-arm estimate, m	x-arm actual, m
1	120	225	0.82	0.8
2	200	195	0.50	0.5
3	255	270	0.57	0.5
4	330	265	-0.08	0
5	400	268	-0.84	-0.8
6	485	220	-1.58	-1.5

Estimated impact point (x-arm l_x) and force direction shows a good agreement with experimental measurement as shown e.g. in Fig. 14. For instance, in the first experiment an impulse to the vessel is given by applying the force whose direction in the body-fixed system is 225° (direction 0 corresponds to the force from bow, direction 180 corresponds to the force from stern). The force (F_x, F_y) is determined from the acceleration measurements (left plot) using the vessel's masses (see Subsect. 3.1); the estimated directions are shown in the middle plot. Similarly, the yaw moment is determined from the measured yaw angular velocity, after which the $l_x \approx 0.82$ is estimated. On the right plot, we compare the actual and estimated moments (l_y is small compared to l_x and is neglected here).

4. A VESSLE'S VELOCITY ESTIMATION AND DEAD RECKONING

Accurate dynamic positioning requires precise measurement of the vessel's velocity, which are not directly available from GPS and other reference sensors (position measurements can be noisy, velocity measurements provided by GPS are not very accurate at low speed). The problem of robust observer design for DP is well studied in the literature (Loria et al., 2000; Fossen and Perez, 2009), falling beyond the scope of our paper.

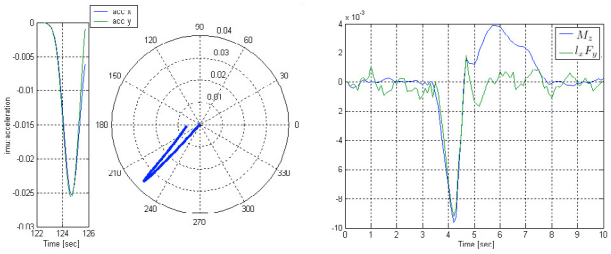

Fig. 14. External force direction and arm estimation.

The velocity estimators can be improved by the results of INS processing in two ways:

- In presence of position measurements, the INS filter can be used as a sufficiently accurate source as velocity. Fig. 15 shows velocity estimates during maneuvers of the icebreaking vessel (Appendix B): we compare the output of INS filter (aided by GPS1) and the velocities given by the two GPS filters.
- In the absence of position measurement (dead reckoning), the "unaided" INS filter can nevertheless predict the vessel's position for several minutes. The quality of prediction depends on the acceleration biases (low-frequency component of the measurement error) $a_0(t), \omega_0(t)$. Results predictions are shown in Fig. 16.

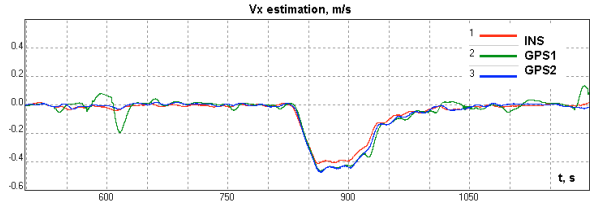

Fig. 15. Sea trials data: velocity estimation

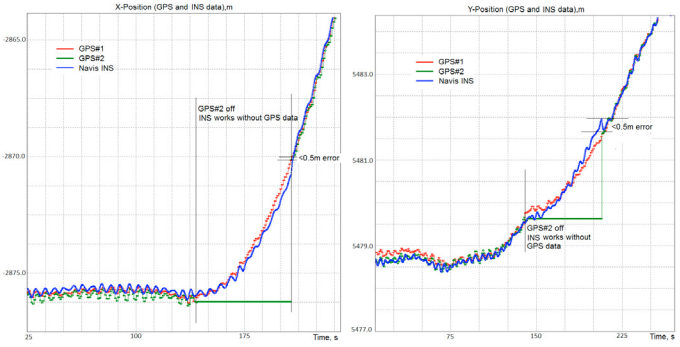

Fig. 16. Two maneuvers with 60s INS prediction (dead reckoning). GPS1 is not fed to INS and used only for comparison; INS is aided solely by GPS2. When GPS2 data is lost, the INS is fed by the last stored measurements of latitude and longitude.

5. CONCLUSION

This research shows benefits of using deep integration of inertial system with DP control system. Commonly, an

INS is considered as a self-standing external device and uses a simplified kinematic model of motion. Its close coupling with a DP controller makes it possible to provide the fusion of all sensors data, using a comprehensive vessel's motion model and other information available to the DP control system. The marriage of INS and DP control system yields a number of benefits such as the external force estimation, sensor fault detection and isolation (based on comparison of measured linear accelerations and angular rates with vessel dynamics model with thrusters forces and moments corrected by IMU data processing), enhanced unaided positioning (dead reckoning). A necessary requirement for the aforementioned applications, however, is the availability of a well-tuned and checked mathematical model of the vessel which is not always possible in practice. With further development of autonomous vessels, which are specially designed for DP operations, the INS sensors could be used widely for autonomous shipping. We are also working on new intelligent sensor devices, meshing INS measurements with data from other positioning references, e.g. GPSs and hydro-acoustic sensors.

6. ACKNOWLEDGEMENTS

The authors are very grateful to their colleagues from Fiber Optical Solutions `http://opticalsolution.lv`, Aker Arctic (`https://akerarctic.fi/`) and Navis Engineering OY (`https://navisincontrol.com`), especially Vyacheslav Fedorov, Reko-Antti Suojanen and Veikko Immonen, Petr Ivanovsky and Timo Karkkainen.

REFERENCES

Guide for Dynamic Positioning Systems. American Bureau of Shipping, Houston, TX, 2013.

V.M. Ambrosovsky and E.B. Ambrosovskaya. Sea trials of high speed crafts: data processing and model identification. In *Int. Conf. on Fast Sea Transportation FAST'2005*, 2005.

Torleiv H. Bryne, R. H. Rogne, T. I. Fossen, and T. A. Johansen. Inertial sensors for risk-based redundancy in dynamic positioning. In *Int. Conf. Ocean, Offshore and Arctic Engineering OMAE 2017*, pages 1–10, 2017.

Torleiv H. Bryne, Robert H. Rogne, Thor I. Fossen, and Tor A. Johansen. A virtual vertical reference concept for aided inertial navigation at the sea surface. *Control Engineering Practice*, 70:1 – 14, 2018. ISSN 0967-0661.

Mark Carter. DP INS – a paradigm shift? In *Dynamic Positioning Conf.*, 2011.

T. I. Fossen and T. Perez. Kalman filtering for positioning and heading control of ships and offshore rigs. *IEEE Control Systems Magazine*, 29(6):32–46, 2009. doi: 10.1109/MCS.2009.934408.

H.F. Grip, Thor I. Fossen, Tor A. Johansen, and Ali Saberi. Globally exponentially stable attitude and gyro bias estimation with application to GNSS/INS integration. *Automatica*, 51:158 – 166, 2015.

Minh-Duc Hua. Attitude estimation for accelerated vehicles using GPS/INS measurements. *Control Engineering Practice*, 18(7):723 – 732, 2010.

A.D. King. Inertial Navigation - Forty Years of Evolution. *GEC Review*, 13(3):140–149, 1998.

A. Loria, T. I. Fossen, and E. Panteley. A separation principle for dynamic positioning of ships: theoretical and experimental results. *IEEE Transactions on Control Systems Technology*, 8(2):332–343, 2000.

V.V. Matveev and V. Ya. Raspopov. *Fundamental principles for design of strapdown inertial navigation systems (in Russian)*. Electropribor, St. Petersburg, 2009.

Yves Paturel. PHINS, an all-in-one sensor for DP applications. In *Dynamic Positioning Conf.*, 2014.

Arne Rinnan, Sverre Bratberg, Nina Gundersen, and Marit Sigmond. Including GNSS based heading in inertial aided GNSS DP reference system. In *Dynamic Positioning Conf.*, 2012.

R. H. Rogne, T. A. Johansen, and T. I. Fossen. Observer and IMU-based detection and isolation of faults in position reference systems and gyrocompasses with dual redundancy in dynamic positioning. In *IEEE Conf. Control Appl. (CCA)*, pages 83–88, 2014.

Robert H. Rogne, Torleiv H. Bryne, Thor I. Fossen, and Tor A. Johansen. Mems-based inertial navigation on dynamically positioned ships: Dead reckoning. *IFAC-PapersOnLine*, 49(23):139 – 146, 2016.

David Russell. Integrating INS and GNSS sensors to provide reliable surface positioning. In *Dynamic Positioning Conf.*, 2012.

R. Stephens, F.Cretollier, P.-Y. Morvan, and A. Chamberlain. Integration of an inertial navigation system and DP. In *Dynamic Positioning Conf.*, 2008.

David H. Titterton and John L. Weston. *Strapdown Inertial Navigation Technology - 2nd Edition*. Inst. of Electrical Engineering, Stevenage, UK, 2004.

K. Vickery. The development and use of an inertial navigation system as a DP position reference sensor (IPRS). In *Dynamic Positioning Conf.*, 1999.

Appendix A. THE IMU SENSOR SPECIFICATION

IFOS-500 communicates with a DP system via RS-422 interface at the baud rate 921600. IFOS-500 provides a proprietary binary interface. To detect delays and dropouts in data, each message contains a timestamps. IFOS-500 provides termo-compensated measurements of linear accelerations a_x, a_y, a_z and angular rates ω_x, ω_y, ω_z (see Fig. 2) at 600Hz frequency. The accuracies reported by the manufacturer are: the acceleration bias drift is $< 0.5 \cdot 10^{-3} g$, angular rate bias drift is $< 0.1^\circ/hour$, and the angle random walk (ARW) is $0.007^\circ/\sqrt{hour}$.

Appendix B. VESSELS' PARTICULARS

The characteristics of the icebreaker vessel are: length overall 121 m, breadth 25 m, displacement 14500 t, bow azimuth thruster 6500 kW, bow tunnel thruster 1800 kW, two stern azimuths each 7500 kW.

The particulars of a vessel model used for towing tank tests (provided by Aker Arctic): length 4.25 m, breadth 1.25 m, displacement 0.95 t, thrusters: one bow and two stern azimuth, each 0.5 kW.